Available online at www.sciencedirect.com
ScienceDirect
Journal of Sound and Vibration 298 (2006) 788–809
JOURNAL OF SOUND AND VIBRATION
www.elsevier.com/locate/jsvi

Apparent mass of seated men—Determination with single- and multi-axis excitations at different magnitudes

Barbara Hinz[a,*], Ralph Blüthner[a], Gerhard Menzel[a], Sebastian Rützel[b], Helmut Seidel[a], Horst Peter Wölfel[b]

[a]*Federal Institute for Occupational Safety and Health, Vibration and Electromagnetic Fields Unit, Nöldnerstr. 40-42, D-10317 Berlin, Germany*
[b]*Department of Structural Dynamics, Darmstadt University of Technology, Petersenstr. 30, D-64287 Darmstadt, Germany*

Received 2 May 2006; received in revised form 10 May 2006; accepted 8 June 2006
Available online 2 August 2006

Abstract

Apparent mass data describing the biodynamic responses of the human body during whole-body vibration in vertical direction using rigid seats has often been published and standardized. Such data has been used as a target function for developing models. At present there is no adequate database for the apparent mass during whole-body vibration in horizontal direction and in more than one vibration axis. Experiments and subsequent data analysis can be used to improve the database for modelling. An experimental study was performed with 13 male subjects sitting on a rigid seat without backrest, and with a hand resting on a support. They were exposed to random whole-body vibration with root-mean square (rms) values of about 0.25, 1.0 and 2.0 m s^{-2} in vertical, fore-and-aft, and lateral direction, and additionally in two horizontal vibration axes and all three vibration axes simultaneously. The forces and accelerations were measured in x-, y-, and z-directions for each condition tested. With an increase of the vibration magnitude in the three directions measured, the apparent mass functions shifted to lower frequencies. At the same vibration magnitude, the apparent mass functions shifted to the lower frequencies with an increasing number of vibration axes. The effects of the factors vibration magnitude and number of axes on the apparent mass curves were tested. The method of the modal description was applied to all individual apparent mass functions in order to obtain representative target functions. Recommendations for the revision of ISO 5982 were summarized.

1. Introduction

The biodynamic response of the seated human body—mainly in the z-direction—has often been evaluated in terms of the driving point impedance or apparent mass in relation to the force and the acceleration at the interface between subject and seat. Such functions can provide the basis for developing mathematical models of the human body and of vibration dummies. The quality of all models can be improved by an extended database for the effects of single-axis vibration and of vibration generated in two or three axes.

*Corresponding author. Tel.: 049 30 51548 4431; fax: 049 30 51548 4170.
E-mail address: Hinz.barbara@baua.bund.de (B. Hinz).

0022-460X/$ - see front matter © 2006 Elsevier Ltd. All rights reserved.
doi:10.1016/j.jsv.2006.06.020

1.1. The effect of vibration magnitude

1.1.1. Single-axis excitation—z-direction

Numerous studies of the apparent mass or impedance of the human body during vibration exposure in z-direction have been published since the early 1950s. The results have been summarized in ISO 5982 [1] and Hinz et al. [2]. Most studies have investigated the frequency range between 0.2 and 20 Hz during sinusoidal or random excitations with intensities between 0.25 and 3 $m\,s^{-2}$ root-mean square (rms). The main resonance peak was consistently found to be approximately 4–5 Hz [2–6], and partially a secondary resonance to be between about 8 and 13 Hz [3,5].

Peak moduli of the apparent mass in the range of 4–5 Hz were reported as decreasing with an increase in excitation magnitude [2,6,7]. Mansfield [8] and Mansfield and Griffin [3] found a general trend of the maximum modulus to increase with rising magnitudes of input. The median of the normalized moduli increased from 1.66 to 1.74 during random vibration with magnitudes from 0.25 to 2.5 $m\,s^{-2}$. The reason for the divergent findings may be the different test conditions of the studies, e.g. the different ranges of the vibration magnitudes and different postures. The seat heights were not reported, but were found to affect the peak magnitude [7]. The individual dependence of the maximum moduli of the apparent mass on the magnitude was reported to be different for various subjects tested [9] and can be considered as one of the main reasons for different findings. Tests with broad-band random inputs (0.125–25 Hz) presented at six magnitudes (0.125; 0.25; 0.4; 0.63; 1.0, 1.6 $m\,s^{-2}$ rms) caused approximately constant peak moduli of the apparent mass during vibration magnitudes higher than 0.40 $m\,s^{-2}$ rms, but with an increase of vibration magnitudes from 0.125 to 0.40 $m\,s^{-2}$ rms, the moduli of the apparent mass at resonance decreased [10]. So far the effects of the vibration magnitude have been described only by changes in the maximum moduli. There are no systematic studies that examine these effects on parameters characterizing the entire apparent mass function.

A consistent finding is the decrease of the peak frequencies with higher vibration magnitudes [2–8,11–14]. This nonlinear behaviour is interpreted as a nonlinear softening effect [12]. In the study of Toward [10], narrowband inputs at 1/2-octave intervals (1–16 Hz) were presented at five magnitudes. The apparent masses of 12 subjects tested were dependent on the frequency of the narrow-band inputs. The magnitude of vibration below 4 Hz had the greatest effect on the modulus of the apparent mass at resonance, while the magnitude of the vibration at frequencies below 8 Hz had the greatest effect on the resonance frequency [10].

1.1.2. Single-axis excitation—x-direction

Some fundamental data on the dynamic response in x-direction has been published since the 1990s. The studies have investigated the frequency range between 0.25 and 20 Hz [15,16] except [17] (frequency range between 0.25 and 80 Hz) during sinusoidal or random excitations with intensities between 0.125 and 2 $m\,s^{-2}$ rms. There is a certain inconsistency in observed modes of the apparent mass.

Fairley and Griffin [15] reported the first mode at 0.7 Hz for sitting on a rigid seat without backrest, hands in the lap with random vibration, and a second one, the main resonance, at 2–2.5 Hz. Holmlund et al. [17] registered for the same posture, but with sinusoidal vibration, one peak modulus between 5 and 6 Hz. With an increase in vibration magnitude, Holmlund et al. [17] observed a decrease in the resonance frequency. In an upright posture (without backrest contact) and with a right angle between upper and lower legs, Nawayseh and Griffin [16] observed three vibration modes: the first around 1 Hz at some vibration magnitudes; the second between 1 and 3 Hz for all 12 subjects and postures tested and most of the vibration magnitudes, and a third between 3 and 5 Hz for 8 of the 12 subjects. These modes varied between subjects, depending on the input magnitude and the height of the foot support. For the condition "average thigh contact" the apparent masses in x-direction shifted towards lower frequencies with increasing vibration magnitude. The maximum moduli and the peak frequencies were lower, when the vibration magnitude increased from 0.125 to 1.25 $m\,s^{-2}$ rms.

With backrest contact the magnitudes of the apparent mass increase, as does the mean resonance frequency [15]. Holmlund and Lundström [18] found a decrease in the peak frequency of the apparent mass around 5 Hz when subjects changed from an erect to a relaxed posture with feet resting on the floor.

To summarize the references the apparent mass in x-direction is influenced by the backrest contact, the muscle tension (posture erect, relaxed), foot support, and thigh contact.

1.1.3. Single-axis excitation—y-direction

In two studies mentioned above the authors also examined the exposure to vibration in the y-direction. Fairly and Griffin [15] registered the first resonance peak of the apparent mass at about 0.7 Hz for both postures, the second one for the posture 'without backrest contact' at around 2 Hz, and 'with backrest contact' at 1.5 Hz. Holmlund and Lundström [18] registered two peaks at around 2 and 6 Hz, where the second peak diminished with increasing vibration (magnitudes between 0.25 and 1.4 $m\,s^{-2}$). In the relaxed posture the second peak (around 6 Hz) decreased with the increasing vibration level. The authors interpreted the human body as a two-mass system at lower vibration levels, but as a one mass system at higher levels.

1.2. Target functions

To obtain representative target functions a summary of individual apparent mass data is required. Usually the summaries were performed by calculating the mean or median values of the apparent mass functions. Some of the authors [3,16,19] noticed a loss of information when averaging the moduli and phases of the apparent mass. This loss of information is described as 'smeared out' by averaging when calculating a mean or median response [16], because not all modes are at the same frequencies in all subjects.

A mean value of the apparent masses calculated by averaging the individual apparent masses of several subjects represents a new system with properties which are different from the individual properties of each subject [2]. Usually only one or two peak values, i.e. two points of the moduli of the apparent mass, were discussed as a function of the vibration magnitude. The whole curves were not considered.

An alternative method of summarizing individual values of the apparent mass function is the approximation of individual curves by modelling [20]—the so-called modal description—of the apparent mass, i.e. the determination of the modal parameters as modal masses, natural frequencies, and damping ratios. This method makes it possible to consider the whole individual curve of the modulus of the apparent mass—expressed in parameters [21]—in the statistical analysis. The combination of this method with an averaging process of the parameters and subsequent calculation of the corresponding average apparent mass function seems to be suitable for deriving target functions, which can reflect more clearly the peak values observed in a group of individuals.

1.3. Aim of the study

To the authors' knowledge possible differences between the apparent mass functions determined during different vibration magnitudes and with a variable number of vibration axes have not been systematically examined. The aim of the study is to examine the biodynamic behaviour with the apparent mass functions as a function of the vibration magnitude and the number of axes during single- and multi-axis vibration. To obtain target functions of the apparent masses for model development, the individual apparent mass functions must be summarized. For this purpose two methods—the usual averaging of the individual apparent mass functions and the averaging of the individual modal parameters—are used.

2. Methods

2.1. Exposure conditions and subjects

The exposures were generated by the control system of the hexapod simulator modified for human experiments. The requirements of ISO 13090-1 [22] were considered. The subjects were exposed to single-axis vibration in X-, Y-, and Z-axis at three vibration magnitudes, dual-axis vibration in X- and Y-axis as well as three-axis vibration in X-, Y-, and Z-axis simultaneously at two vibration magnitudes. The excitation axes are marked by capitals, but measuring directions by lower-case letters (e.g. a Xx means acceleration measured in x-direction during the excitation in X axis). The subjects were exposed to random whole body vibration (nearly flat spectrum from 0.25 to 30 Hz for 60 s) with unweighted rms values (Table 1, Fig. 1). The twofold presentation of the vibration magnitudes and directions was balanced across the subjects.

Table 1
Minimum, maximum, mean values ($N = 26$) and standard deviations (SD) for the root-mean square values (rms) of the unweighted input accelerations a [m s^{-2}] measured in x-, y-, and z-direction during single-axis (X, Y, Z), dual-axis (XY), and three-axis (XYZ) excitations and the vector sums of the dual- and three-axis excitations

	Minimum	Maximum	Mean	SD
Exposure 1 (E1)				
rms *a X x*	0.256	0.381	0.284	0.021
rms *a XY x*	0.244	0.275	0.259	0.011
rms *a XYZ x*	0.246	0.284	0.265	0.012
rms *a Y y*	0.244	0.341	0.287	0.028
rms *a XY y*	0.241	0.275	0.257	0.012
rms *a XYZ y*	0.242	0.278	0.259	0.012
rms *a Z z*	0.250	0.269	0.259	0.006
rms *a XYZ z*	0.237	0.251	0.243	0.004
vector sum *XY xy*	0.343	0.466	0.380	0.029
vector sum *XYZ xyz*	0.346	0.536	0.431	0.052
Exposure 2 (E2)				
rms *a X x*	0.983	1.183	1.069	0.071
rms *a XY x*	0.840	0.948	0.888	0.038
rms *a XYZ x*	0.858	0.986	0.916	0.042
rms *a Y y*	0.887	1.111	0.987	0.076
rms *a XY y*	0.814	0.941	0.870	0.041
rms *a XYZ y*	0.835	0.966	0.897	0.042
rms *a Z z*	0.810	0.850	0.829	0.012
rms *a XYZ z*	0.780	0.813	0.795	0.010
vector sum *XY xy*	1.173	1.618	1.327	0.118
vector sum *XYZ xyz*	1.176	1.827	1.477	0.191
Exposure 3 (E3)				
rms *a X x*	1.836	2.138	1.978	0.103
rms *a Y y*	1.724	2.023	1.849	0.097
rms *a Z z*	1.552	1.594	1.575	0.013

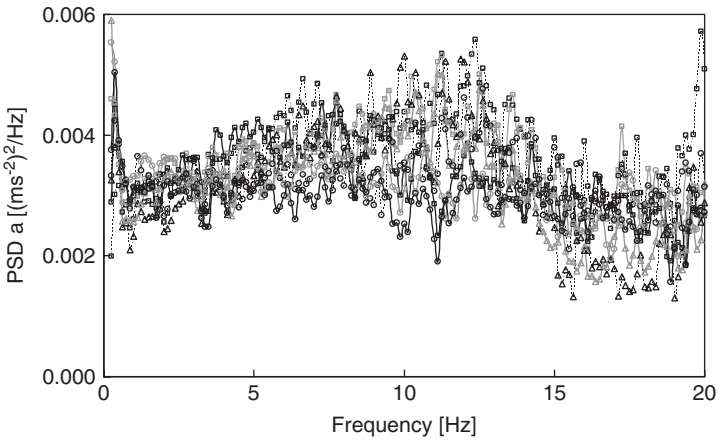

Fig. 1. Mean values of power spectral densities (PSD) of the input accelerations with the lowest vibration magnitude E1: …… x-direction, y-direction, z-direction, □ single-axis excitation X, Y, Z, △ dual-axis excitation XY, ○ three-axis excitation.

An experimental study was performed with 13 male subjects with body masses between 61.3 and 103.6 kg (mean value (MV) 79.3 kg), and body heights between 173.5 and 197.0 cm (MV 183.5 cm). A total of 26 anthropometric parameters in the standing and 12 parameters in the sitting posture were measured [23]. The

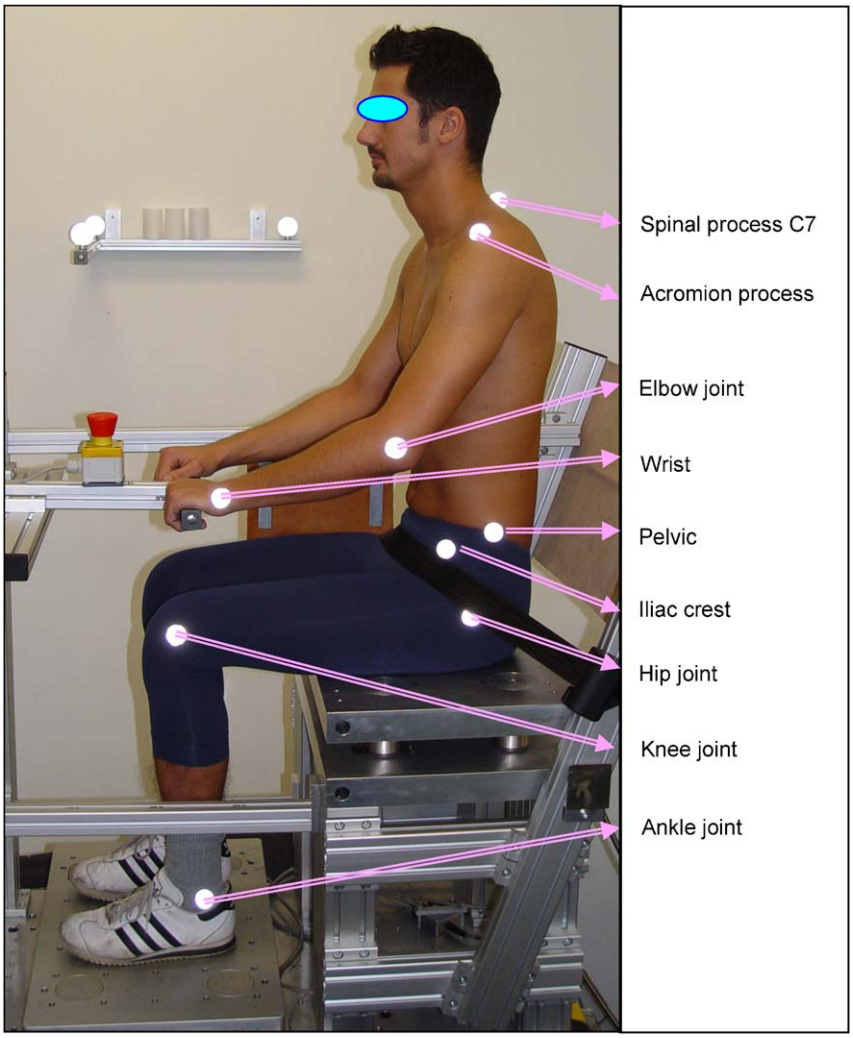

Fig. 2. The experimental situation is illustrated by the photography of a male subject sitting on a rigid seat with an integrated force plate and instrumented by markers of the motion analysis.

subjects sat on the force plate (Fig. 2), which was integrated in a rigid seat, with their ischial tuberosities approximately 20–30 cm from the front edge of the force plate and with the hands on a support. They were asked to adopt a comfortable, upright posture with normal muscle tension for the duration of each test. The feet were supported on a plate, 48.5 cm below the top surface of the force plate with lower legs nearly vertical. For safety reasons a hip belt was used.

2.2. Data acquisition

A force plate (Kistler 9396 AB) capable of measuring forces in three directions simultaneously was mounted as seat surface in order to measure forces in the fore-and-aft (x) direction, lateral (y) direction and vertical (z) direction. The force plate ($60 \times 40 \times 20$ cm) consisted of four tri-axial quartz piezoelectric transducers of the same sensitivity located at the four corners of the plate. Signals from the force plate were amplified using an eight-channel amplifier (Kistler 9865 B). The time series of forces were corrected by subtracting the product of the mass of the plate resting on the force sensors and the acceleration measured at the seat plate for all conditions tested. This method was verified by measurements with rigid masses on the plate.

Accelerations in three translational directions (x, y, and z) were measured at the force plate in each test using three capacitance accelerometers (ENDEVCO 7290A-10) mounted on a special block for them (ENDEVCO 7990 block). The block was fixed on the right side of the Kistler force plate. The data acquisition was performed by a WaveBook (WBK16, Iotech).

A motion analysis system (Qualisys) was used to register the movements of body points (spinal process of C7, acromion process, elbow joint, wrist, pelvic, iliac crest, hip joint, knee joint, and ankle—see Fig. 2).

2.3. Data processing

The forces in the three translational directions were related to the input accelerations in the same direction. The complete transfer matrix [24] or cross-axis apparent masses [16] are beyond the scope of this paper.

The apparent mass (AM) is defined as the complex ratio of force amplitude (F) and acceleration amplitude (a) in the same direction (x, y, z) as a function of frequency (f). The apparent mass was calculated by the cross spectral density method using a MatLab routine.

$$AMx(f) = \frac{Fx(f)}{ax(f)}, \quad AMy(f) = \frac{Fy(f)}{ay(f)}, \quad AMz(f) = \frac{Fz(f)}{az(f)}. \tag{1}$$

The associated coherency was calculated as

$$\gamma^2(Fx, ax) = \frac{|Fxax(f)|^2}{Fx(f)ax(f)}, \; \gamma^2(Fy, ay) = \frac{|Fyay(f)|^2}{Fy(f)ay(f)}, \; \gamma^2(Fz, az) = \frac{|Fzaz(f)|^2}{Fz(f)az(f)}. \tag{2}$$

The moduli of the apparent mass were normalized by dividing the latter by the static mass on the platform in the posture tested. The mean values of the moduli of the individual apparent masses were calculated by the usual averaging method.

For each individual normalized apparent mass function the maximum modulus and its location, i.e. peak frequency, were determined for statistical analysis.

The influence of the factors vibration magnitude, number of axes, and repetition on the maxima of the moduli of the apparent masses and their frequencies were tested by the general linear model (GLM) Repeated Measures procedure (SPSS PC—analysis of variance, when the same measurement is made several times on the same subject). The GLM Repeated Measures procedure provides both univariate and multivariate analysis including the Bonferroni post hoc test. The Bonferroni test, based on Student's statistic, adjusts the observed significance level to take account of the fact that multiple comparisons of mean values are made.

2.4. Target functions

The human body can be represented as model, which contains a base mass m_0 [kg] and n sets of single degree of freedom (dof) structures consisting of a mass, a spring and a damper. This approach implies linearity of the system.

The apparent mass of the model can be calculated with the excitation frequency $f = \Omega/2\pi$ as

$$M(\Omega) = m_0 + \sum_{r=1}^{n} m_r \frac{1 + \mathrm{j}2s_r(\Omega/\omega_r)}{1 - (\Omega/\omega_r)^2 + \mathrm{j}2s_r(\Omega/\omega_r)} \tag{3}$$

modal masses m_r [kg], natural frequencies $f_r = \omega_r/(2\pi)$ [Hz], damping ratios $s_r = c_r/(2\sqrt{m_r k_r})$ [dimensionless].

To obtain representative target functions, the individual apparent mass functions were approximated by models with a suitable number of dof to identify the main peaks. The identification algorithm is based on the minimization of error functions expressed in terms of apparent mass errors [21].

Each apparent mass function can be represented by a model which contains a base mass m_0 [kg] (the minimum of m_0 was limited at 0.1 kg) and n sets of single dof structures. The number of sets in a model coincides with the number of peaks in the apparent mass function to be approximated. The sets are determined by the modal parameters: modal masses m_r, natural frequencies f_r and damping ratios s_r ($r = 1 \ldots n$).

Two sets of single dof structures ($n = 2$) were used to identify the apparent masses in the horizontal directions x and y in the range between 0.25 and 20 Hz. Three peaks were identified and three sets of single dof

structures ($n = 3$; set 1: f_1, s_1, m_1; set 2: f_2, s_2, m_2; set 3: f_3, s_3, m_3) were determined to approximate the apparent mass curves in vertical direction in the range between 0.25 and 30 Hz.

The influences of the factors vibration magnitude, number of axes, and repetition on the sets of parameters were tested by the GLM Repeated Measures procedure (SPSS PC). The GLM Repeated Measures multivariate analysis was applied to all sets describing the complete apparent mass function as well as to each set separately reflecting the range of one peak.

The mean curves of the modelled apparent mass functions were obtained on the basis of the mean values of the parameters for each condition tested. They can be considered as a target function.

3. Results

Very small differences were registered between the apparent masses of the 13 subjects at frequencies above 10 Hz. The apparent mass functions of the horizontal directions were presented in Fig. 3 and in all following figures in the range between 0 and 10 Hz to show more clearly the course of the functions in the low frequency range. Furthermore the apparent mass was very small at some frequencies above 10 Hz and the estimate of phase was likely to be inaccurate. The apparent mass functions of the vertical direction were illustrated in the figures in the range between 0 and 20 Hz.

3.1. Single-axis excitation

3.1.1. Excitation in X-axis, measurements in x-direction (X x)

The mean curves of the modulus of the normalized apparent mass determined by usual averaging show a clear dependence on the vibration magnitude for the single axis vibration (Fig. 3(a), Fig. 4(a)). The different amounts of shifts towards the lower frequencies are proportional to the differences of the levels of exposure intensities. The values of the coherency functions were in the range between 0.6 and 0.99 with the lower values at the higher frequencies.

The mean peak moduli and also the normalized mean peak moduli (Table 2) remained nearly unchanged across the intensities and directions. The main peak frequencies decreased with the increasing vibration magnitude from 2.94 to 2.18 Hz (Table 3). A second peak was registered for most subjects in the range around 1 Hz (see Fig. 4(a)—individual curves). The usual process of averaging produced a plateau rather than a peak, because the second peak was relatively small and occurred at slightly different frequencies in each individual curve (see Fig. 4(a)—mean values).

The multivariate analyses showed a significant influence exerted by the vibration magnitude on both variables tested—the main peak modulus and the peak frequency of the apparent mass—whereas the repetition had no influence (Table 4). The univariate analysis showed no systematic dependence of the maximum moduli of the apparent mass on the vibration magnitude. The differences of mean values between the vibration magnitudes tested (E1/E2, E1/E3, E2/E3) were also not significantly different (Table 5). The peak frequencies decreased with increasing vibration magnitude. The differences in mean values of the peak frequencies were significant between all vibration magnitudes tested (Table 5).

3.1.2. Excitation in Y-axis, measurements in y-direction (Y y)

The mean curves of the normalized moduli of the apparent masses, calculated by usual averaging, show a clear dependence on the vibration magnitude for the single-axis vibration (Fig. 3(b)). A second smaller peak occurred below 1 Hz (Fig. 4(b)). The curves suggest that the modulus of the main peak decreased, whereas the peak below 1 Hz increased with increasing vibration magnitude. With the highest vibration magnitude the two peaks seem to merge to form a plateau.

The coherency functions showed values in the range between 0.6 and 0.96 with the lower values at the higher frequencies.

The normalized mean peak moduli remained nearly unchanged (Table 2). The frequency at which the normalized main peak values occurred decreased from 2.04 to 1.37 Hz with rising vibration magnitude (Table 3).

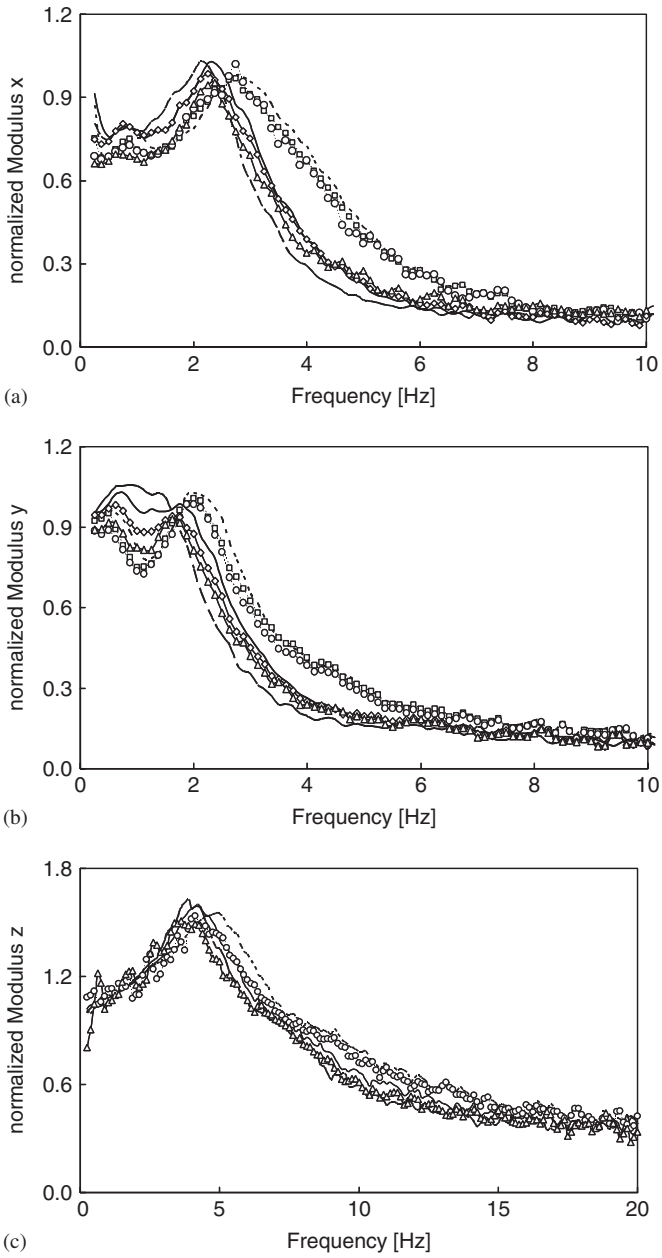

Fig. 3. Mean values of the normalized moduli of the apparent mass function: (a) in x-direction, (b) in y-direction, (c) in z-direction. …… vibration magnitude E1, ——— vibration magnitude E2, — ▪ — vibration magnitude E3, 'no marker' single-axis excitation X, Y, Z, □ dual-axis excitation XY E1, ○ three-axis excitation E1, ◇ dual-axis excitation XY E2, △ three-axis excitation XYZ E2.

The multivariate analyses showed a significant influence exerted by the vibration magnitude on both the main peak modulus and the peak frequency of the apparent mass, whereas the repetition had no effect (Table 4). The univariate analysis showed no systematic dependence of the maximum moduli of the apparent mass on the vibration magnitude. The peak frequencies were significantly influenced by the factor vibration magnitude, and the differences in mean values were significantly different between all vibration magnitudes tested (Table 5).

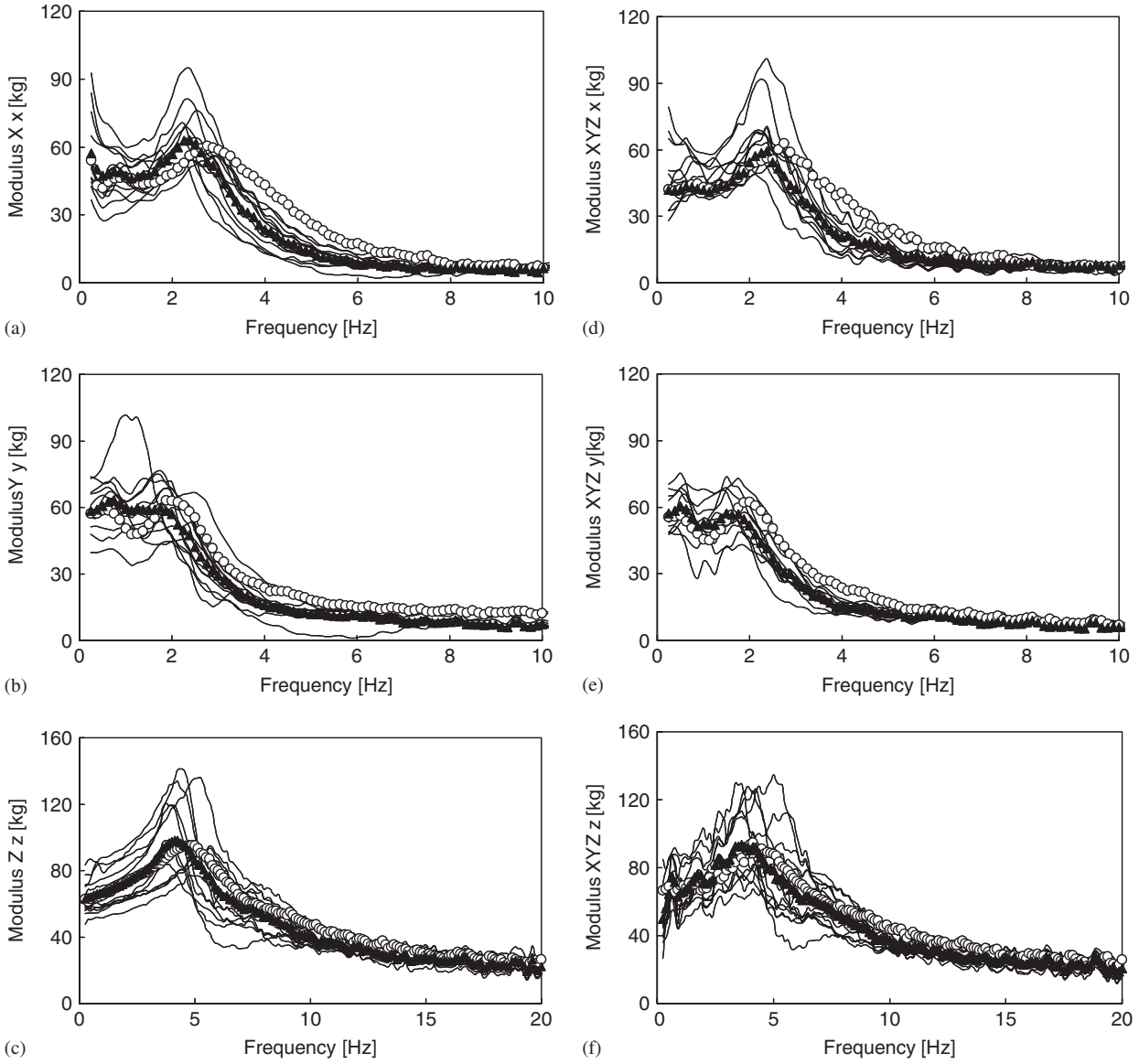

Fig. 4. Moduli of the apparent mass functions: (a) x-direction during single-axis excitation X, (b) y-direction during single-axis excitation Y, (c) z-direction during single-axis excitation Z, (d) x-direction during three-axis excitation XYZ, (e) y-direction during three-axis excitation XYZ, (f) z-direction during three-axis excitation XYZ. …… individual values during the vibration magnitude E1, ▬ individual moduli during the vibration magnitude E2, ○ mean modulus during the vibration magnitude E1, ▲ mean modulus during the vibration magnitude E2.

3.1.3. Excitation in Z-axis, measurements in z-direction (Z z)

The mean curves of the normalized moduli and phases of the apparent mass show a clear dependence on the vibration magnitude for the single-axis vibration (Fig. 3(c)). For the coherency function, values between 0.9 and 0.99 were registered in the whole frequency range tested. The normalized mean peak moduli remained nearly unchanged (Table 2) and their location fell with the increasing vibration magnitude from 5.14 to 4.41 Hz (see Table 3). A few subjects produced a small peak below 1 Hz. In the individual curves a further peak in the range between 10 and 12 Hz was observed (Fig. 4(c)). The averaged mean curves cannot reflect these peaks sufficiently.

Table 2
Minimum, maximum, mean values ($N = 26$) and standard deviations (SD) for the maximum (max.) moduli of the apparent mass function ($|AM|$) and of the normalized moduli of the apparent mass function (norm. $|AM|$)| in x-, y-, and z-direction during single-axis (X, Y, Z), dual-axis (XY), and three-axis (XYZ) excitations with the vibration magnitudes E1, E2, and E3

	Minimum	Maximum	Mean	SD
Exposure 1 (E1)				
Max. $\|AM\|$ X x	48.44	86.11	63.34	10.43
Max. $\|AM\|$ XY x	48.58	85.99	62.39	9.58
Max. $\|AM\|$ XYZ x	46.47	95.51	64.13	13.59
Max. $\|AM\|$ Y y	42.00	90.40	67.01	12.76
Max. $\|AM\|$ XY y	40.90	97.04	65.18	14.49
Max. $\|AM\|$ XYZ y	36.88	97.51	64.33	14.95
Max. $\|AM\|$ Z z	74.82	141.64	104.29	21.79
Max. $\|AM\|$ XYZ z	70.60	131.98	102.15	19.23
Exposure 2 (E2)				
Max. $\|AM\|$ X x	50.31	96.37	66.16	11.99
Max. $\|AM\|$ XY x	46.33	93.15	64.28	12.54
Max. $\|AM\|$ XYZ x	26.61	100.93	65.18	17.66
Max. $\|AM\|$ Y y	44.65	100.52	63.71	13.65
Max. $\|AM\|$ XY y	42.09	92.34	60.06	11.97
Max. $\|AM\|$ XYZ y	38.79	88.38	59.83	11.77
Max. $\|AM\|$ Z z	68.58	141.30	107.21	21.38
Max. $\|AM\|$ XYZ z	67.15	134.68	102.51	20.35
Exposure 3 (E3)				
Max. $\|AM\|$ X x	45.60	93.76	66.02	11.71
Max. $\|AM\|$ Y y	44.11	88.12	64.82	12.55
Max. $\|AM\|$ Z z	69.67	145.70	107.47	22.26
Exposure 1 (E1)				
Max. norm. $\|AM\|$ X x	0.78	1.24	1.06	0.11
Max. norm. $\|AM\|$ XY x	0.77	1.24	1.04	0.11
Max. norm. $\|AM\|$ XYZ x	0.83	1.32	1.06	0.13
Max. norm. $\|AM\|$ Y y	0.75	1.49	1.12	0.19
Max. norm. $\|AM\|$ XY y	0.78	1.46	1.08	0.19
Max. norm. $\|AM\|$ XYZ y	0.74	1.47	1.07	0.20
Max. norm. $\|AM\|$ Z z	1.43	2.13	1.72	0.17
Max. norm. $\|AM\|$ XYZ z	1.47	1.96	1.69	0.12
Exposure 2 (E2)				
Max. norm. $\|AM\|$ X x	0.89	1.32	1.10	0.11
Max. norm. $\|AM\|$ XY x	0.82	1.31	1.07	0.12
Max. norm. $\|AM\|$ XYZ x	0.74	1.31	1.07	0.19
Max. norm. $\|AM\|$ Y y	0.69	1.37	1.06	0.17
Max. norm. $\|AM\|$ XY y	0.66	1.39	1.00	0.16
Max. norm. $\|AM\|$ XYZ y	0.64	1.33	1.00	0.17
Max. norm. $\|AM\|$ Z z	1.41	2.31	1.78	0.20
Max. norm. $\|AM\|$ XYZ z	1.46	1.98	1.69	0.14
Exposure 3 (E3)				
max. norm. $\|AM\|$ X x	0.80	1.39	1.10	0.15
Max. norm. $\|AM\|$ Y y	0.75	1.33	1.07	0.14
Max. norm. $\|AM\|$ Z z	1.15	2.08	1.77	0.13

The multivariate analyses showed a significant influence exerted by the vibration magnitude on both the main peak modulus and the peak frequency of the apparent mass, whereas the repetition exerted no influence (Table 4). The univariate analysis exhibited no significant effects of the vibration magnitude on the maximum moduli of the apparent mass. The frequency at which the maximum peak occurred decreased significantly with the increasing vibration magnitude (Tables 4 and 5).

Table 3
Minimum, maximum, mean values ($N = 26$) and standard deviations (SD) for the frequencies (f) at which the maximum (max.) normalized (norm.) moduli of the apparent mass function ($|AM|$) occurred in x-, y-, and z-direction during single-axis (X, Y, Z), dual-axis (XY), and three-axis (XYZ) excitations with the vibration magnitudes E1, E2, and E3

	Minimum	Maximum	Mean	SD
Exposure 1 (E1)				
f (max. norm. $\|AM\|$) X x	2.38	4.00	2.94	0.42
f (max. norm. $\|AM\|$) XY x	2.00	4.50	2.94	0.57
f (max. norm. $\|AM\|$) XYZ x	2.00	4.00	2.82	0.46
f (max. norm. $\|AM\|$) Y y	1.13	2.75	2.04	0.31
f (max. norm. $\|AM\|$) XY y	1.63	2.75	2.11	0.29
f (max. norm. $\|AM\|$) XYZ y	1.75	2.75	2.19	0.29
f (max. norm. $\|AM\|$) Z z	3.38	6.63	5.14	0.96
f (max. norm. $\|AM\|$) XYZ z	3.13	6.25	4.71	0.89
Exposure 2 (E2)				
f (max. norm. $\|AM\|$) X x	1.75	3.00	2.45	0.28
f (max. norm. $\|AM\|$) XY x	1.13	3.00	2.29	0.36
f (max. norm. $\|AM\|$) XYZ x	1.25	4.00	2.40	0.44
f (max. norm. $\|AM\|$) Y y	1.13	2.38	1.62	0.32
f (max. norm. $\|AM\|$) XY y	1.13	2.38	1.66	0.38
f (max. norm. $\|AM\|$) XYZ y	1.13	2.25	1.61	0.29
f (max. norm. $\|AM\|$) Z z	3.5	5.88	4.69	0.77
f (max. norm. $\|AM\|$) XYZ z	3.38	5.63	4.31	0.85
Exposure 3 (E3)				
f (max. norm. $\|AM\|$) X x	1.63	2.50	2.18	0.19
f (max. norm. $\|AM\|$) Y y	1.13	1.75	1.37	0.19
f (max. norm. $\|AM\|$) Z z	3.25	5.63	4.41	0.69

Table 4
Results (p-values) of the multi- and univariate analyse (GLM Repeated Measures) to test the effects of the factors vibration magnitude, repetition, and the number of axes on the maximum moduli of the apparent mass function (max.$|AM|$) and on its frequency (f(max.$|AM|$)) in x-, y-, and z-direction during single-axis (X, Y, Z), dual-axis (XY), and three-axis (XYZ) excitations (significance level $p<0.05$, the factor vibration magnitude was tested at 2 or 3 levels (e2, e3), the factor number of axes at 2 or 3 levels (d2, d3), and the factor repetition at 2 levels (r2))

Conditions tested (factors with level)	Multivariate			Univariate					
				max. $\|AM\|$			f(max.$\|AM\|$)		
	Vibration magnitude	Repetition	Number of axes	Vibration magnitude	Repetition	Number of axes	Vibration magnitude	Repetition	Number of axes
x-direction									
X x (e3, r2)	0.000	0.795	—	0.570	0.537	—	0.000	0.895	—
XY x (e2, r2, d2)	0.000	0.777	0.004	0.054	0.777	0.001	0.000	0.940	0.224
XYZ x (e2, r2, d3)	0.000	0.708	0.295	0.121	0.406	0.426	0.000	0.771	0.218
y-direction									
Y y (e3, r2)	0.000	0.289	—	0.530	0.123	—	0.000	0.754	—
XY y (e2, r2, d2)	0.000	0.442	0.062	0.001	0.376	0.033	0.000	0.455	0.334
XYZ y (e2, r2, d3)	0.000	0.482	0.025	0.004	0.334	0.008	0.000	0.411	0.318
z-direction									
Z z (e3, r2)	0.000	0.105	—	0.152	0.878	—	0.000	0.030	—
XYZ z (e2, r2, d2)	0.000	0.188	0.004	0.216	0.958	0.047	0.000	0.063	0.001

Table 5
Results (p values) of the Bonferroni post hoc test to test the significance level of differences between the mean values for the two or three levels of the factors vibration magnitude (top) and number of axes (bottom)

Conditions tested (factors with level)	max|AM|			f(max|AM|)		
Factor vibration magnitude						
x-direction	E1/E2	E1/E3	E2/E3	E1/E2	E1/E3	E2/E3
X x (e3, r2)	n	n	n	.000*	.000*	.000*
XY x (e2, r2, d2)	.054	—	—	.000*	—	—
XYZ x (e2, r2, d3)	n	—	—	.000*	—	—
y-direction	E1/E2	E1/E3	E2/E3	E1/E2	E1/E3	E2/E3
Y y (e3, r2)	.070	.070	n	.000*	.000*	.000*
XY y (e2, r2, d2)	.001*	—	—	.000*	—	—
XYZ y (e2, r2, d3)	.004*	—	—	.000*	—	—
z-direction	E1/E2	E1/E3	E2/E3	E1/E2	E1/E3	E2/E3
Z z (e3, r2)	n	n	n	.001*	.000*	.000*
XYZ z (e2, r2,d2)	n	—	—	.001*	—	—
Factor number of axes						
x-direction	X x/XY x	X x/XYZ x	XY x/XYZ x	Xx/XY x	Xx/XYZ x	XY x/XYZ x
XY x (e2, r2, d2)	.001*	—	—	n	—	—
XYZ x (e2, r2, d3)	.004*	n	n	n	n	n
y-direction	Y y/XY y	Y y/XYZ y	XY y/XYZ y	Y y/XY y	Y y/XYZ y	XY y/XYZ y
XY y (e2, r2, d2)	.033*	—	—	n	—	—
XYZ y (e2, r2, d3)	.050*	.050*	n	n	n	n
z-direction	—	Z z/XYZ z	—	—	Z z/XYZ z	—
XYZ z (e2, r2,d2)	—	.047*	—	—	.001*	—

(Maximum modulus of the apparent mass (max.|AM|) and the peak frequency (f(max.|AM|)) in x-, y-, and z-direction with single-axis (X, Y, Z), dual-axis (XY), and three-axis (XYZ) excitations with the vibration magnitudes E1, E2, and E3 (*—significance level $p<0.05$; n—non-significant difference).

3.2. Dual-axis excitation

3.2.1. Excitation in X and Y axes, measurements in x-direction (XY x)

3.2.1.1. Vibration magnitude. The averaged mean curves of the normalized moduli and phases of the apparent mass showed a similar dependence on the vibration magnitude to that with the single-axis vibration (Fig. 3(a)). The coherency functions had values between 0.6 and 0.99 with the lower values at higher frequencies.

The normalized mean peak moduli showed a small increase (0.03) with the vibration magnitude (Table 2) and their location changed with the increasing vibration magnitude from 2.94 to 2.29 Hz (Table 3). The second peak around 1 Hz was also registered.

The results of the statistical analysis covering the lowest and the medium vibration magnitude did not differ from those of the single-axis excitations (Tables 4 and 5).

3.2.1.2. Number of axes. Within each vibration magnitude a minor shift of the curves of the modulus of the apparent mass towards lower frequencies can be observed with a changeover from single- to dual-axis of excitation (Fig. 3 (a)—within E1 and within E2).

The normalized mean peak moduli were slightly higher during single-axis excitation than during dual-axis excitation for each exposure tested (Table 2). When the excitation changed from one to two axes, the mean peak frequencies remained nearly unchanged during the lowest exposure E1, but the mean peak frequencies decreased during the higher exposure E2 (Table 3).

The multivariate analyses showed a significant influence exerted by the number of axes on both the maximum moduli and the peak frequencies whereas the univariate analyses revealed a significant influence

exerted by the number of axes on the maximum moduli, but not on the peak frequencies (Table 4). The differences between the mean values of the maximum moduli during the single- and dual-axis excitations were significant, those of the peak frequencies were not (Table 5).

3.2.2. Excitation in X and Y axes, measurements in y-direction (Xy y)

3.2.2.1. Vibration magnitude. The averaged mean curves of the normalized moduli and phases of the apparent mass showed a similar dependence on the vibration magnitude to that during the single-axis vibration (Fig. 3(b)). A second smaller peak also occurred below 1 Hz. With rising vibration magnitude the moduli of the main peak decreased, whereas the peak below 1 Hz increased. The coherency functions showed values in the range between 0.6 and 0.96 with the lower values at higher frequencies.

With the rising vibration magnitude the normalized mean peak moduli decreased from 1.08 to 1.00 (Table 2), the main peak frequency shifted from 2.11 to 1.66 Hz (Table 3, Fig. 3(b)).

The multivariate analyses showed a significant influence exerted by the vibration magnitude on both the main peak modulus and the peak frequency of the apparent mass, whereas the repetition exerted no influence (Table 4). The univariate analysis revealed a significant influence exerted by the vibration magnitude on the maximum moduli of the apparent mass and the frequencies of their occurrence. The mean values of both variables were significantly different during the vibration magnitudes E1 and E2 (Table 5).

3.2.2.2. Number of axes. Within each vibration magnitude (E1 and E2) a moderate shift in the curves of the moduli of the apparent mass towards the lower frequencies are observed with the dual-axis excitation (Fig. 3(b)—within E1 and within E2). The normalized mean peak moduli were higher during single-axis excitation than during dual-axis excitation within each exposure tested (Table 2). A change from the single- to dual-axis input produced non-systematic changes in the mean peak frequencies during the two exposures tested (Table 3).

As the multivariate analysis has shown, the influence of the number of axes on the set consisting of the maximum modulus and the peak frequency is not significant, but the p-value 0.062 is relatively low (Table 4). The univariate analysis showed a significant influence exerted by the number of axes on the maximum moduli, but not on the peak frequencies. Also the results of the post hoc tests indicate significant differences between the mean values of the maximum moduli during single- and dual-axis excitations (Table 5).

3.3. Three-axes excitation

3.3.1. Excitation in X, Y, and Z axes, measurements in x-direction (XYZ x)

3.3.1.1. Vibration magnitude. The averaged mean curves of the normalized moduli and phases of the apparent mass showed a similar dependence on the vibration magnitude to that during the single axis vibration (Fig. 3(a)). The values of the coherency functions were in the range between 0.6 and 0.99 with the lower values at the higher frequencies. The normalized mean peak moduli remained almost unchanged during the vibration magnitude tested (Table 2) and occurred between 2.82 Hz (low vibration magnitude) and 2.40 Hz (Table 3). The second peak around 1 Hz was also registered (Fig. 4(d)).

The results of the statistical analysis covering the lowest and the medium vibration magnitude did not differ from those of the single- and dual-axis excitations (Tables 4 and 5).

3.3.1.2. Number of axes. Within each exposure tested a minor shift in the curves of the modulus of the apparent mass with the increase of the number of excitation axes towards lower frequencies is observed (Fig. 3(a)—within E1 and within E2).

The maximum peak frequencies (Table 3) decreased when the input was changed from single- to three-axis vibration during the exposure with the lowest (E1) and medium (E2) vibration magnitude. Within both vibration magnitudes tested the maximum moduli of the apparent mass in x-direction (Table 2) were lower when the number of input axis increased from one to two.

When the numbers of input axes were expanded from two to three, the maximum moduli of the apparent mass in x-direction increased during E1, but remained constant during E2.

The number of axes had no significant effect on the variables maximum moduli and peak frequencies, either in the multivariate or in the univariate analysis (Tables 4 and 5).

3.3.2. Excitation in X, Y, and Z axes, measurements in y-direction (XYZ y)

3.3.2.1. Vibration magnitude. The mean curves of the moduli and phases of the apparent mass showed a similar dependence on the vibration magnitude to that during the single-axis vibration (Figs. 3(b), 4(e)). A second smaller peak also occurred below 1 Hz. With the rising vibration magnitude the moduli of the main peak decreased, whereas the second peak increased. The coherency functions showed values in the range between 0.6 and 0.96 with lower values at higher frequencies. With rising vibration magnitude the normalized mean peak moduli decreased from 1.07 to 1.00 (Table 2), and the main peak frequency changed from 2.19 to 1.61 Hz (Table 3).

The statistical analysis covering the lowest and the middle vibration magnitude produced similar results to those for the dual-axis excitations (Tables 4 and 5).

3.3.2.2. Number of axes. Within each exposure tested a moderate shift in the curves of the modulus, and for E1, in the phases of the apparent mass is observed with increase of the number of excitation axes to the lower frequencies (Fig. 3(b)—within E1 and within E2).

The maximum moduli of the apparent mass in *y*-direction (Table 2) were significantly lower when the numbers of axes were increased from one to two and from two to three (Table 5). The peak frequencies shifted towards higher frequencies when a second axis was added (Table 3). When the third axis was supplemented, the peak frequency increased within E1 and decreased within E2.

The multivariate analysis delivered a significant effect of the factor number of axes on the set consisting of the maximum moduli and the peak frequencies (Table 4). The univariate analysis showed a significant influence exerted by the number of axes on the maximum moduli, but not on the peak frequencies.

3.3.3. Excitation in X, Y, and Z axes, measurements in z-direction (XYZ z)

3.3.3.1. Vibration magnitude. The averaged mean curves of the normalized moduli and phases of the apparent mass show for the single-axis vibration a clear dependence on the vibration magnitude (Fig. 3(c)). Values in the range between 0.9 and 0.99 were registered for the coherency function in the whole frequency range tested. The normalized mean peak moduli remained nearly unchanged with the increasing vibration magnitude (Table 2), but the mean peak frequency decreased from 4.71 to 4.31 Hz (Table 3). In some individual curves a second peak in the range between 6 and 10 Hz is observed (Fig. 4(f)). The mean curves calculated by averaging do not reflect these peaks.

The multivariate analyses showed a significant influence exerted by the vibration magnitude on the set consisting of the main peak modulus and the main frequency of the apparent mass, whereas the repetition had no influence (Table 4). The maximum moduli of the apparent mass remained almost constant with the two intensities tested. The univariate analysis (Table 4) and the non-significant differences of mean values (Table 5) confirmed this result. The frequency at which the maximum peak occurred decreased significantly with the increasing vibration magnitude (Tables 4 and 5).

3.3.3.2. Number of axes. The curves of the modulus of the apparent mass shifted towards the lower frequencies, when the single-axis excitation (*Z*) only was compared with the excitation in three directions (*XYZ*), (Fig. 3(c)—within E1 and within E2).

The normalized mean peak moduli (Table 2) and the peak frequencies (Table 3) were clearly lower during the three-axis excitation than during the single-axis excitation (Table 2). In the individual curves a second peak was observed in the range between 10 and 12 Hz. The additional peaks described for the single-axis excitation (Fig. 4(c)) were also registered in the individual curves during the three axes excitation (Fig. 4(f)). The peak below 1 Hz may be due to several causes during the three-axis vibration: the pure effect of the vibration in *Z*-axis or the additional effect of the excitation in horizontal directions (*X*, *Y*). The mean curves do not reflect these peaks.

The multivariate analysis delivered a significant effect of the factor number of axes on the set consisting of the maximum moduli and peak frequencies (Table 4).

During both vibration magnitudes tested (E1, E2), the maximum moduli and peak frequencies decreased significantly (Table 5), when the number of axes increased from one to three.

3.4. Target functions

Each individual apparent mass curve was approximated by a model which contained a base mass and 2 or 3 sets of single dof structures for the horizontal directions and the vertical, respectively. The range of the main peaks determined by the conventional method coincides with the range of set 2 in the x- and in the y-direction, and with set 1 in the z-direction (Tables 3 and 6). Further peaks observed in the individual curves were identified (Table 6) for the x-direction in the range between 1.1 and 2.2 Hz (set 1), for the y-direction between 0.7 and 1.4 Hz (set 1), and for the z-direction between 6.6 and 10.6 Hz (set 2).

The multivariate statistical analysis was applied to all sets of modal parameters and to each set separately. Both the vibration magnitude and the number of axes exert significant influence on all sets or on all modal parameters together which represent the apparent mass function during the three-axis vibration in all three directions and the dual-axis vibration in y-direction (Table 7). Application of the multivariate statistical analysis to each set of modal parameters representing ranges of the apparent mass characterized by a peak value reveals significant effects of the factor vibration magnitude on all three sets and of the factor number of axes on set 2 during the three-axis excitations in y-direction and on set 3 in z-direction. A clear tendency towards the same effect on set 2 during the dual- and three-axis excitation in x-direction is indicated by p values of 0.056 and 0.051.

On the basis of the mean values of the parameters ($N = 13$) of each condition tested, the curves of the mean apparent mass functions were obtained (Fig. 5). To compare the apparent masses determined with two methods, the differences in terms of 'mean apparent mass derived from the mean values of modal parameters of the individual models' minus 'mean apparent mass determined as usual by averaging the individual curves point by point in each bandwidth' were calculated. The results reveal clear differences. For the horizontal directions the maximum differences amounted to 12 kg in the frequency range below 4 Hz, whereas above 4 Hz the differences were clearly lower. In the vertical direction the differences reflected the underestimation of the peak values by the normal averaging process, i.e. around 5 and 10 Hz. Systematic differences between the single-axis and the three-axis excitation were not obvious. In particular all peaks are more distinct in the apparent mass curves based on the modal description. Their location often deviates from those resulting from the usual averaging (Fig. 5).

4. Discussion

4.1. Single-axis excitation

4.1.1. Excitation in X-axis, measurements in x-direction (X x)

The results from this study during single-axis vibration show similar features to those previously reported. At around 2 Hz a maximum magnitude of about 60 kg was identified [19] and at 2.5 Hz the main resonance was found with individual maximum moduli between 50 and 76 kg (see Fig. 1 in [15]). For the posture with average thigh contact, median moduli were observed between about 75 and 60 kg in the frequency range between 2 and 6 Hz [16] with the highest values during the lowest vibration magnitude ($0.125\,\mathrm{m\,s^{-2}}$). The maximum moduli of the apparent mass of this study were found between 62 and 66 kg at frequencies between 2.18 and 2.94 Hz.

Further peaks were detected around 1 Hz [15,16] and 5–6 Hz [16–19]. But the authors mentioned, that these peaks were not permanently observed, either at different vibration magnitudes or in all subjects. In the data of this study, a first peak was registered around 1 Hz and the second was the maximum peak around 3 Hz. Several peaks were found only for some of the subjects, mainly with the lowest vibration magnitude. The mean values reflect these peaks inadequately.

In this study the maximum moduli increased with the increasing body mass and decreased with an increasing chest circumference in the subjects. Fairley and Griffin [15] discuss the fact that the peak moduli

Table 6
Lower and upper bound of the 95% confidence intervals (CI), mean values and standard errors (Std. error) for the natural frequencies f_1, f_2, f_3 of the corresponding sets of the modal description of the apparent mass functions $|AM|$ in x-, y-, and z-direction during single-axis (X, Y, Z), dual-axis (XY), and three-axis (XYZ) excitations based on the modal identification. Vibration magnitudes: E1, E2, E3 ($N = 26$)

	Lower bound of the 95% CI	Upper bound of the 95% CI	Mean value	Std. error
Exposure 1 (E1)				
f_1 ($\|AM\|$) X x	1.59	2.16	1.87	0.13
f_1 ($\|AM\|$) XY x	1.48	2.14	1.81	0.15
f_1 ($\|AM\|$) XYZ x	1.60	2.21	1.91	0.14
f_2 ($\|AM\|$) X x	3.02	3.56	3.29	0.12
f_2 ($\|AM\|$) XY x	2.90	3.50	3.20	0.13
f_2 ($\|AM\|$) XYZ x	2.95	3.56	3.26	0.14
f_1 ($\|AM\|$) Y y	0.75	1.11	0.93	0.08
f_1 ($\|AM\|$) XY y	0.86	1.40	1.13	0.12
f_1 ($\|AM\|$) XYZ y	0.87	1.19	1.03	0.07
f_2 ($\|AM\|$) Y y	2.12	2.46	2.29	0.07
f_2 ($\|AM\|$) XY y	1.98	3.02	2.50	0.23
f_2 ($\|AM\|$) XYZ y	2.14	2.60	2.37	0.10
f_1 ($\|AM\|$) Z z	4.83	5.78	5.30	0.21
f_1 ($\|AM\|$) XYZ z	4.75	5.61	5.21	0.20
f_2 ($\|AM\|$) Z z	8.99	10.57	9.78	0.36
f_2 ($\|AM\|$) XYZ z	9.21	10.45	9.83	0.28
f_3 ($\|AM\|$) Z z	18.96	23.38	21.17	1.01
f_3 ($\|AM\|$) XYZ z	20.42	23.61	22.02	0.73
Exposure 2 (E2)				
f_1 ($\|AM\|$) X x	1.16	1.67	1.41	0.11
f_1 ($\|AM\|$) XY x	1.14	1.66	1.40	0.12
f_1 ($\|AM\|$) XYZ x	1.12	1.59	1.36	0.10
f_2 ($\|AM\|$) X x	2.42	2.69	2.55	0.06
f_2 ($\|AM\|$) XY x	2.36	3.22	2.77	0.20
f_2 ($\|AM\|$) XYZ x	2.44	2.77	2.60	0.07
f_1 ($\|AM\|$) Y y	0.81	1.04	0.93	0.05
f_1 ($\|AM\|$) XY y	0.76	0.84	0.80	0.01
f_1 ($\|AM\|$) XYZ y	0.79	0.88	0.83	0.02
f_2 ($\|AM\|$) Y y	1.75	2.11	1.93	0.08
f_2 ($\|AM\|$) XY y	1.98	3.02	2.50	0.23
f_2 ($\|AM\|$) XYZ y	1.79	1.99	1.86	0.06
f_1 ($\|AM\|$) Z z	4.42	5.40	4.91	0.22
f_1 ($\|AM\|$) XYZ z	4.25	5.15	4.70	0.20
f_2 ($\|AM\|$) Z z	7.82	9.31	8.60	0.32
f_2 ($\|AM\|$) XYZ z	7.66	9.23	8.44	0.35
f_3 ($\|AM\|$) Z z	20.53	24.86	22.70	0.99
f_3 ($\|AM\|$) XYZ z	20.36	23.95	22.15	0.82
Exposure 3 (E3)				
f_1 ($\|AM\|$) X x	1.15	1.68	1.41	0.12
f_2 ($\|AM\|$) X x	1.84	3.74	2.79	0.43
f_1 ($\|AM\|$) Y y	0.77	1.01	0.89	0.05
f_2 ($\|AM\|$) Y y	1.32	2.63	1.97	0.30
f_1 ($\|AM\|$) Z z	4.01	4.89	4.48	0.18
f_2 ($\|AM\|$) Z z	6.58	8.28	7.43	0.39
f_3 ($\|AM\|$) Z z	19.33	23.66	21.49	0.99

arose from a forwards and backwards rocking motion of the whole upper body. These motions could be influenced by the mass of the upper body as reflected partially by the chest circumference. The results indicate lower maximum moduli of the apparent mass with increased chest circumferences.

Table 7
Results (p values) of the multivariate analysis (GLM Repeated Measures) to test the effects of the factors vibration magnitude, repetition, the number of axes on the parameters of all sets, and on the parameters of the sets 1, 2, 3 of the modal description of the apparent mass functions in x-, y- and z-direction during single-axis (X, Y, Z), dual-axes (XY), and three-axis (XYZ) excitations (significance level $p<0.05$, the factor vibration magnitude was tested at 2 or 3 levels (e2, e3), the factor number of axes at 2 or 3 levels (d2, d3), and the factor repetition at 2 levels (r2))

Conditions tested level of factors	Multivariate analysis											
	All sets			Set 1 (f_1 s_1 m_1)			Set 2 (f_2 s_2 m_2)			Set 3 (f_3 s_3 m_3)		
	Vibration magnitude	Repetition	Number of axes	Vibration magnitude	Repetition	Number of axes	Vibration magnitude	Repetition	Number of axes	Vibration magnitude	Repetition	Number of axes
x-direction												
X x (e3, r2)	0.003	0.729	—	0.000	0.207	—	0.000	0.827	—	—	—	—
XY x (e2, r2, d2)	0.014	0.560	0.084	0.000	0.348	0.813	0.001	0.799	0.056	—	—	—
XYZ x (e2, r2, d3)	0.003	0.704	0.030	0.001	0.319	0.537	0.001	0.833	0.051	—	—	—
y-direction												
Y y (e3, r2)	0.000	0.058	—	0.002	0.019	—	0.000	0.021	—	—	—	—
XY y (e2, r2, d2)	0.005	0.009	0.006	0.000	0.161	0.172	0.000	0.276	0.101	—	—	—
XYZ y (e2, r2, d3)	0.001	0.008	0.002	0.000	0.043	0.179	0.000	0.273	0.041	—	—	—
z-direction												
Z z (e3, r2)	0.010	0.409	—	0.000	0.175	—	0.000	0.024	—	0.000	0.513	—
XYZ z (e2, r2, d2)	0.004	0.525	0.001	0.000	0.549	0.083	0.003	0.022	0.141	0.000	0.698	0.000

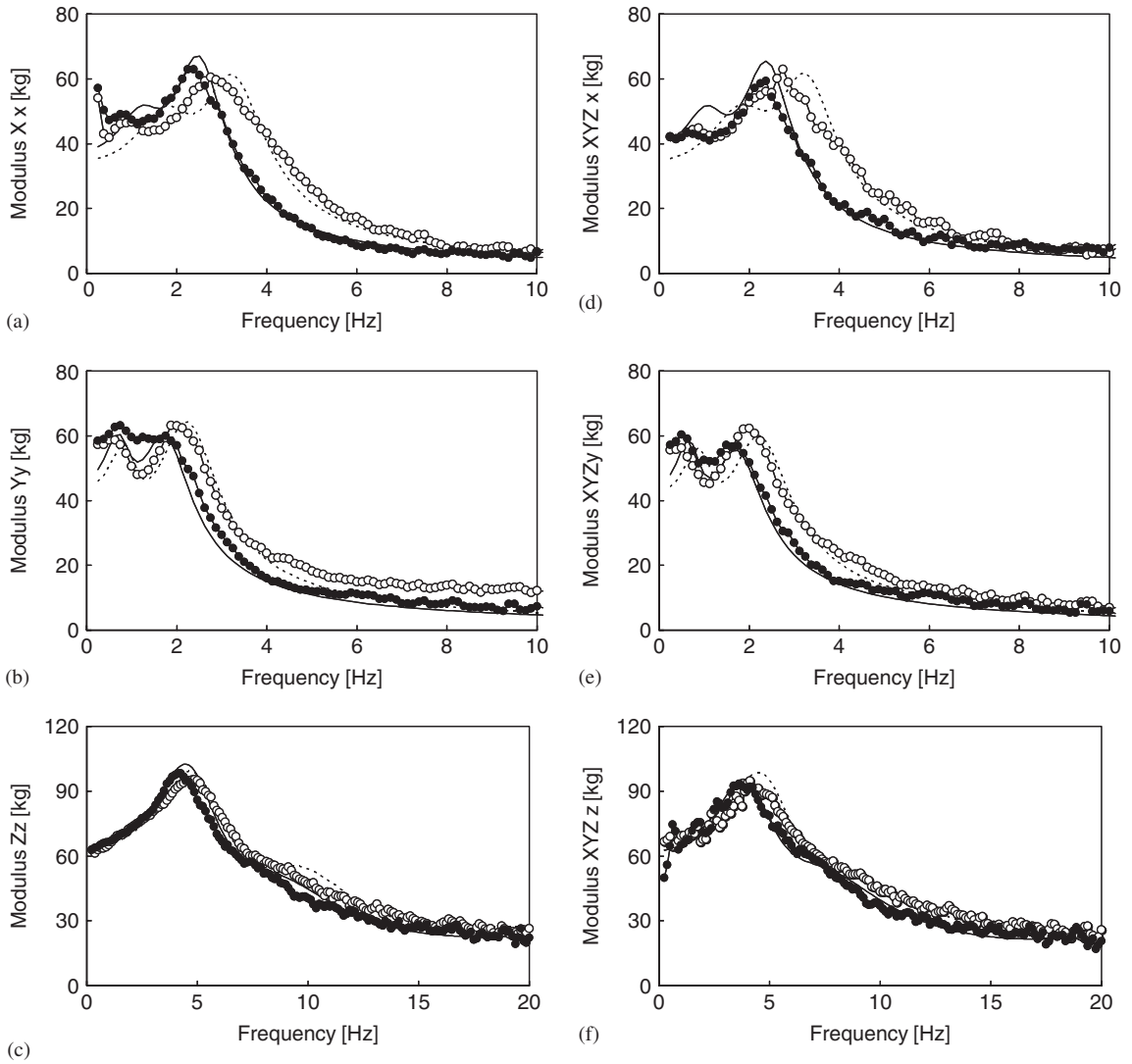

Fig. 5. Mean values of the moduli of the apparent masses: (a) x-direction during single-axis excitation X, (b) y-direction during single-axis excitation Y, (c) z-direction during single-axis excitation Z, (d) x-direction during three-axis excitation XYZ, (e) y-direction during three-axis excitation XYZ, (f) z-direction during three axis excitation XYZ. …… mean values based on the results of the modal description during E1, ▬▬ mean values based on the results of the modal description during E2, ○ mean values calculated by usual averaging during E1, ● values calculated by usual averaging during E2.

4.1.2. Excitation in Y-axis, measurements in y-direction (Y y)

The maximum moduli of the apparent mass of this study were found between 60 and 67 kg at frequencies between 1.61 and 2.19 Hz for the excitation in one direction. These results for the apparent masses during the exposure in y-direction agreed well with data published so far [15,18,19].

A further peak below 1 Hz was observed during the vibration magnitudes E1 and E2 with all conditions tested. A similar pattern was described by Fairley and Griffin [15] who registered the peaks around 1 Hz at the low level exposure. Holmlund and Lundström [18] found the peaks at 2 and 6 Hz. The slightly higher frequencies reported by Holmlund and Lundström [18] are possibly caused by the sinusoidal inputs and the stationary feet. During the highest exposures tested ($2\,m\,s^{-2}$ which correspond to E3), only one wide peak appeared around 1 Hz in the data of this study in agreement with the previous results [15,18]. These findings

could support the assumption of Holmlund and Lundström [18] that the body acts as a two-mass system during low vibration magnitudes and as a one-mass system at higher magnitudes. During the vibration in y-direction the upper body was observed to sway from side to side as already discussed by Fairly and Griffin [15]. The buttocks and pelvis seem to be out of phase with the upper body and the shoulders. The phase lag could disappear due to a higher muscle tension at the higher vibration magnitude so that the whole upper body acts as a single mass. The results give some support to this assumption. During the low intensity tested the iliospinal height and different sizes of the chest and shoulders were related to the maximum moduli of the apparent mass in y-direction, but not the body mass. Only during the exposure with the highest vibration magnitude E3 did the body mass affect the peak modulus in the apparent mass function.

4.1.3. Excitation in Z-axis, measurements in z-direction (Z z)

The apparent masses are of similar shape to those observed by other authors [3,4,8,9,10–12]. The normalized peak moduli of the apparent mass were found to be between 1.2 and 1.9 [9], between 1.6 and 1.7 [3], or between 1.67 and 1.76 [8] during random input vibration up to about 20 Hz and with intensities in the range between 0.125 and 2.5 $m\,s^{-2}$. The normalized peak moduli of this study varied between 1.15 and 2.31 (Table 2) during the three vibration magnitudes tested. With increasing vibration magnitude (between 0.25 and 2.0 or 2.5 $m\,s^{-2}$ rms), an increase or constancy in the peak magnitude were reported by other authors [3,8,9].

The peak frequency of the apparent mass in z-direction decreased from about 6 to 4 Hz, with a vibration magnitude increasing from 0.25 to 2.5 $m\,s^{-2}$ [3,4,9,11]. Holmlund et al. [11] and Mansfield and Griffin [3] describe the occurrence of second peaks with similar properties in the range between 8 and 12 Hz, Towards [10] between 8 and 15 Hz. The second peak is not observed in all subjects and may be considered as an individual property [3]. In some of the individual apparent mass moduli, second peaks around 10 Hz are also observed in this study (Fig. 4(c)). These peaks are not evident in the median data [3] or mean values (Fig. 3(c)).

4.2. Dual- and three-axis excitation

4.2.1. Vibration magnitude

The apparent mass curves during vibration exposures with more than one axis showed general similar dependencies on the frequency to those of the apparent masses during single-axis excitation. It is known that increases in the vibration magnitude produce a decrease in peak frequencies of the apparent mass. Differences between the vibration magnitudes E1 and E2 as well as E2 and E3 were found between 0.6 and 0.8 $m\,s^{-2}$ unweighted rms in all directions measured during the exposures with the number of excitation axis from 1 to three. These differences between the vibration magnitudes caused a shift in the mean peak frequencies in the range between 0.4 and 0.7 Hz. Within the dual-axes and within the three-axis excitation, the dependence of the apparent mass on the vibration magnitude seems to be nearly the same as for the single-axis excitation.

4.2.2. Number of axes

To the authors' knowledge a comparison between the apparent mass values during an increasing number of vibration excitation directions has not been discussed sofar. The results showed that the apparent mass functions in the three measuring directions shifted to lower frequencies when the number of excitation axes increased. This phenomenon could have been caused by an increase of the vibration magnitude or a changing posture from erect to relaxed. The simultaneous effect of the vibration magnitudes in more than one excitation axis may be related to a vector sum (see Table 1). The differences between the rms values during the single-axis excitation and the vector sum of rms values during the dual-axis vibration were for E1 in the range of 0.1 $m\,s^{-2}$, and for E2 in the range of 0.3 $m\,s^{-2}$. These differences were obviously too small to cause significant changes of the peak frequencies in the apparent mass. The differences between the rms values during the single-axis excitation and the vector sum of rms values during the three-axis vibration were for E1 in the range of 0.16 $m\,s^{-2}$, and for E2 in the range of 0.5 to 0.8 $m\,s^{-2}$. These differences are in the same range as those between the vibration magnitudes tested in this study. A corresponding shift of the apparent mass towards lower frequencies was observed only in z-direction: the differences between the peak frequencies of the apparent masses obtained during the conditions of single- and three-axis excitations amounted to 0.43 Hz for

E1 and 0.38 Hz for E2 in z-direction. Hence the increase in the vibration magnitude expressed as vector sum for exposures with more than one excitation axis could well be related to the significant shift of the peak frequencies in z-direction. On the contrary, the different vector sums of single- and multi-axis exposures do not correlate with magnitude-related frequency shifts in the apparent mass in horizontal directions. Further influences may have caused the missing reactions in the horizontal direction.

The effect of the hand support is not clear in detail. The forces acting on the hand support possibly affected the biodynamic behaviour of the human body, predominantly in the x- and y-directions. The combinations of the axes XZ and YZ were not tested in this study. Future results of such exposures could help to elucidate possible different effects of dual-axis excitations in the horizontal and combined horizontal-vertical axes.

The observed movement of the upper body during single-axis excitation, e.g. forwards and backwards rocking motion [15] during fore-and aft vibration, or the relative motions between the lower trunk (buttocks and pelvis) and the upper trunk including the shoulders [15] during lateral vibration, may lead to a combined motion of the body during multi-axis vibration, together with changed dynamic contact conditions at the seat interface. Possibly, the complex motion presented went along with a different pattern of muscle activity and changed dynamic material properties of the soft tissue. Further studies of the effect of these internal body properties on the vibration behaviour of subjects are required to identify the cause of the nonlinearity associated with the number of axes.

4.3. Target functions

The apparent mass functions were generally used as target functions for developing mathematical models, e.g. finite element models, as well as for designing dummies, e.g. for crash tests and seat testing. Only in individual cases was the development of a model aimed at approximating the dynamic properties of one individual subject.

In ISO 5982 [1], the mean maximum modulus of the target functions was obtained from numerous studies and amounts to 75.4 kg, the maximum being 107.6 kg and the minimum 59.9 kg at 4 Hz, regardless of the vibration magnitude. The values of this study (Table 2) suggest higher peak moduli of the apparent mass. One main reason for these differences could be the conventional averaging process, which acts as a smoothing procedure. This effect becomes more pronounced with the number of averaged individual curves, then subsequently leading to smaller peak values. Thus several typical features of individual characteristic curves are eliminated by averaging.

The approximation of each individual apparent mass function by a number of sets permits the identification of relevant main peaks in each individual curve and their description by a number of sets, each with four parameters. The essential information of the apparent mass function expressed by parameter sets can be included in comprehensive statistical analyses to find out the effects of factors, such as the vibration magnitude or the number of vibration axes as tested in this study, on the entire apparent mass function as well as on single characteristics. The results of those statistical analyses can help to quantify target functions better and to gain insight into possible mechanisms.

The mean apparent masses function of a group of subjects obtained from mean values of the modal parameters reflects the peak values more distinctly than the conventional averaging methods. The differences between the mean curves calculated by the two methods described can be assumed to increase with the number of apparent mass curves involved. Application of the modal description can be recommended as basis for a qualitative improvement in the summarizing of apparent mass data, e.g. in a future revision procedure for ISO 5982.

5. Conclusions

The results of the experimental study yield a first database for the development of mathematical models as well as for vibration dummies, taking into account the vibration magnitude, the vibration direction, and the number of vibration axes acting simultaneously. They are limited to the exposure conditions and the range of the subjects' anthropometric data.

The peak frequencies of the apparent mass functions were significantly lower with the increased vibration magnitude. This nonlinearity was found during single-axis vibration as well as during the dual-axis and three-axis vibrations.

A significant shift in peak frequencies of the apparent mass functions in the z-direction was also caused by additional horizontal vibration in x- and y-directions. In both horizontal directions there were comparable tendencies. Hence, an evaluation of dual- or three-axis vibration should consider these interactions, i.e. an isolated assessment of each axis would not appear to be adequate. Further studies are needed to confirm these findings.

The nonlinearities of the apparent mass functions are probably caused by a complex combination of factors, which were not quantified by the measuring technique available. Such factors could include the tissue dynamics at the interface between subject and seat, the relative motions within the body and the active response of muscles. Further studies should be performed with further combinations of axes.

The application of the modal description to the individual apparent mass functions permits a parametric description of the entire apparent mass function and can help to overcome (1) the limited possibilities of analysing the apparent mass functions by statistical tests and (2) the smoothing effect of averaging the individual curves point-wise. The target functions obtained from the modal description reflect the original individual peaks more clearly. The application of the modal description can be recommended as basis for improving and quantifying of representative apparent mass data, e.g. in a future revision procedure for ISO 5982.

Acknowledgements

This research is supported by the European Commission under the Framework 5 Quality of Life and Management of Living Resources Programme—Project No. QLK4-2002-02650 (VIBRISKS).

The authors wish to thank for their support Dr. J. Keitel, Dr. M. Schust, and Dipl.-Ing. Gericke.

References

[1] International Organization for Standardization ISO 5982, Mechanical vibration and shock—range of idealized values to characterize seated-body biodynamic response under vertical vibration, 2001.

[2] B. Hinz, H. Seidel, G. Menzel, R. Blüthner, On the variability of the impedance depending on the intensity, posture and body mass, *Zeitschrift für Arbeitswissenschaft* 55 (2001) 7–14.

[3] N.J. Mansfield, M.J. Griffin, Non-linearities in apparent mass and transmissibility during exposure to whole-body vertical vibration, *Journal of Biomechanics* 33 (2000) 933–941.

[4] Y. Matsumoto, M.J. Griffin, Non-linear characteristics in the dynamic responses of seated subjects exposed to vertical whole-body vibration, *Journal of Biomechanical Engineering* 124 (2002) 527–529.

[5] S. Rakheja, I. Stiharu, P.-É. Boileau, Seated occupant apparent mass characteristics under automotive postures and vertical vibration, *Journal of Sound and Vibration* 253 (2002) 57–75.

[6] B. Hinz, H. Seidel, G. Menzel, L. Gericke, R. Blüthner, J. Keitel, Seated occupant apparent mass in automotive posture—examination with groups of subjects characterised by a representative distribution of body mass and body height, *Zeitschrift für Arbeitswissenschaft* 58 (2004) 250–264.

[7] W. Wang, S. Rakheja, P.-É. Boileau, Effects of sitting postures on biodynamic response of seated occupants under vertical vibration, *International Journal of Industrial Ergonomics* 34 (2004) 289–306.

[8] N. Mansfield, The apparent mass of the human body in the vertical direction—the effect of the magnitude, *Proceedings of the UK Informal Group Meeting Conference on Human Response to Vibration*, Alverstoke, September 1994, pp. 1–13.

[9] T.E. Fairley, M.J. Griffin, The apparent mass of the seated human body: vertical vibration, *Journal of Sound and Vibration* 22 (1989) 81–94.

[10] M.G.R. Toward, Apparent mass of the human body in vertical direction: effect of input spectra, *Proceedings at the 37th United Kingdom Conference on Human Response to Vibration*, Loughborough, September 2002, pp. 67–75.

[11] P. Holmlund, R. Lundström, L. Lindberg, Mechanical impedance of the human body in vertical direction, *Applied Ergonomics* 31 (2000) 415–422.

[12] Y. Matsumoto, M.J. Griffin, Effect of muscle tension on non-linearities in the apparent masses of seated subjects exposed to vertical whole-body vibration, *Journal of Sound and Vibration* 253 (2002) 77–92.

[13] N. Nawayseh, M.J. Griffin, Non-linear dual-axis biodynamic response to vertical whole-body vibration, *Journal of Sound and Vibration* 268 (2003) 503–523.

[14] M.G.R. Toward, Apparent mass of the seated human body in the vertical direction: effect of holding a steering wheel, *Proceedings of the 39th United Kingdom Group Meeting on Human Response to Vibration*, Ludlow 15–17 September 2004, pp. 211–221.
[15] Fairly, M.J. Griffin, The apparent mass of the seated human body in the fore-and-aft and lateral directions, *Journal of Sound and Vibration* 139 (1990) 299–306.
[16] N. Nawayseh, M.J. Griffin, Non-linear dual-axis biodynamic response to fore-and-aft whole-body vibration, *Journal of Sound and Vibration* 282 (2005) 831–862.
[17] P. Holmlund, R. Lundström, L. Lindberg, Mechanical Impedance of the human body during horizontal vibration exposure, *Proceedings of International Conference on Whole-body Vibration Injuries*, Southampton, September 1997, pp. 35–36.
[18] P. Holmlund, R. Lundström, Mechanical impedance of the human body in horizontal direction, *Journal of Sound and Vibration* 215 (1998) 801–812.
[19] N.J. Mansfield, R. Lundström, The apparent mass of the human body exposed to non-orthogonal horizontal vibration, *Journal of Biomechanics* 32 (1999) 1269–1278.
[20] L. Wei, M.J. Griffin, Mathematical models for the apparent mass of the seated human body exposed to vertical vibration, *Journal of Sound and Vibration* 212 (1998) 855–874.
[21] S. Rützel, B. Hinz, H.P. Wölfel,. Modal Description—a better way of characterising human vibration behaviour, *Journal of Sound and Vibration*, 2005, in press, doi:10.1016/j.jsv.2006.06.019.
[22] International Organization for Standardization ISO 13090-1, Mechanical vibration and shock—Guidance on safety aspects of tests and experiments with people—part 1: exposure to whole-body vibration and shock, 1998.
[23] H.-J. Wilke, P. Neef, B. Hinz, H. Seidel, L. Claes, Intradiscal pressure together with anthropometric data—a data set for the validation of models, *Clinical Biomechanics* 16 (2001) S111–S126.
[24] S.D. Smith, J.A. Smith, R.J. Newman, C.M. Loyer, Multi-axis vibration transmission characteristics of occupied suspension seats, *Proceedings of the 38th UK Conference on Human Response to Vibration*, Alverstoke, September 2003, 13p.